ARL

US Army Research Laboratory

Photoacoustic Spectroscopy for Trace Vapor Detection and Standoff Detection of Explosives

by Ellen L Holthoff, Logan S Marcus, and Paul M Pellegrino

NOTICES

Disclaimers

(12 pt) The findings in this report are not to be construed as an official Department of the Army position unless so designated by other authorized documents.

Citation of manufacturer's or trade names does not constitute an official endorsement or approval of the use thereof.

Destroy this report when it is no longer needed. Do not return it to the originator.

ARL

US Army Research Laboratory

Photoacoustic Spectroscopy for Trace Vapor Detection and Standoff Detection of Explosives

by Ellen L Holthoff and Paul M Pellegrino
Sensors and Electron Devices Directorate, ARL

Logan S Marcus
Oak Ridge Associated Universities, Oak Ridge, TN

REPORT DOCUMENTATION PAGE

1. REPORT DATE *(DD-MM-YYYY)*	2. REPORT TYPE	3. DATES COVERED (From - To)
August 2016	Reprint	

4. TITLE AND SUBTITLE	5a. CONTRACT NUMBER
Photoacoustic Spectroscopy for Trace Vapor Detection and Standoff Detection of Explosives	
	5b. GRANT NUMBER
	5c. PROGRAM ELEMENT NUMBER

6. AUTHOR(S)	5d. PROJECT NUMBER
Ellen L Holthoff, Logan S Marcus, and Paul M Pellegrino	
	5e. TASK NUMBER
	5f. WORK UNIT NUMBER

7. PERFORMING ORGANIZATION NAME(S) AND ADDRESS(ES)	8. PERFORMING ORGANIZATION REPORT NUMBER
US Army Research Laboratory ATTN: RDRL-SEE-E 2800 Powder Mill Road Adelphi, MD 20783-1138	ARL-RP-0577

9. SPONSORING/MONITORING AGENCY NAME(S) AND ADDRESS(ES)	10. SPONSOR/MONITOR'S ACRONYM(S)
	11. SPONSOR/MONITOR'S REPORT NUMBER(S)

12. DISTRIBUTION/AVAILABILITY STATEMENT

Approved for public release; distribution is unlimited.

13. SUPPLEMENTARY NOTES

14. ABSTRACT

The Army is investigating several spectroscopic techniques (e.g., infrared spectroscopy) that could allow for an adaptable sensor platform. Current sensor technologies, although reasonably sized, are geared to more classical chemical threats, and the ability to expand their capabilities to a broader range of emerging threats is uncertain. Recently, photoacoustic spectroscopy (PAS), employed in a sensor format, has shown enormous potential to address these ever-changing threats. PAS is one of the more flexible IR spectroscopy variants, and that flexibility allows for the construction of sensors that are designed for specific tasks.

PAS is well suited for trace detection of gaseous and condensed media. Recent research has employed quantum cascade lasers (QCLs) in combination with MEMS-scale photoacoustic cell designs. The continuous tuning capability of QCLs over a broad wavelength range in the mid-infrared spectral region greatly expands the number of compounds that can be identified. We will discuss our continuing evaluation of QCL technology as it matures in relation to our ultimate goal of a universal compact chemical sensor platform. Finally, expanding on our previously reported photoacoustic detection of condensed phase samples, we are investigating standoff photoacoustic chemical detection of these materials. We will discuss the evaluation of a PAS sensor that has been designed around increasing operator safety during detection and identification of explosive materials by performing sensing operations at a standoff distance. We investigate a standoff variant of PAS based upon an interferometric sensor by examining the characteristic absorption spectra of explosive hazards collected at 1 m.

15. SUBJECT TERMS

photoacoustic spectroscopy, sensor, quantum cascade laser, MEMS, laser Doppler vibrometer, standoff, explosives detection

16. SECURITY CLASSIFICATION OF:			17. LIMITATION OF ABSTRACT	18. NUMBER OF PAGES	19a. NAME OF RESPONSIBLE PERSON
			UU	14	Ellen L Holthoff
a. REPORT	b. ABSTRACT	c. THIS PAGE			19b. TELEPHONE NUMBER (Include area code)
Unclassified	Unclassified	Unclassified			301-394-0939

Photoacoustic Spectroscopy for Trace Vapor Detection and Standoff Detection of Explosives

Ellen L. Holthoff, Logan S. Marcus, and Paul M. Pellegrino

U.S. Army Research Laboratory, 2800 Powder Mill Road, RDRL-SEE-E, Adelphi, MD, USA 20783

ABSTRACT

The Army is investigating several spectroscopic techniques (e.g., infrared spectroscopy) that could allow for an adaptable sensor platform. Current sensor technologies, although reasonably sized, are geared to more classical chemical threats, and the ability to expand their capabilities to a broader range of emerging threats is uncertain. Recently, photoacoustic spectroscopy (PAS), employed in a sensor format, has shown enormous potential to address these ever-changing threats. PAS is one of the more flexible IR spectroscopy variants, and that flexibility allows for the construction of sensors that are designed for specific tasks.

PAS is well suited for trace detection of gaseous and condensed media. Recent research has employed quantum cascade lasers (QCLs) in combination with MEMS-scale photoacoustic cell designs. The continuous tuning capability of QCLs over a broad wavelength range in the mid-infrared spectral region greatly expands the number of compounds that can be identified. We will discuss our continuing evaluation of QCL technology as it matures in relation to our ultimate goal of a universal compact chemical sensor platform. Finally, expanding on our previously reported photoacoustic detection of condensed phase samples, we are investigating standoff photoacoustic chemical detection of these materials. We will discuss the evaluation of a PAS sensor that has been designed around increasing operator safety during detection and identification of explosive materials by performing sensing operations at a standoff distance. We investigate a standoff variant of PAS based upon an interferometric sensor by examining the characteristic absorption spectra of explosive hazards collected at 1 m.

Keywords: Photoacoustic spectroscopy, sensor, quantum cascade laser, MEMS, laser Doppler vibrometer, standoff, explosives detection

1. INTRODUCTION

There will always be a critical need for detection and identification of hazardous materials. In recent years, photoacoustic spectroscopy (PAS) has emerged as an attractive and powerful technique well suited for sensing applications. PAS techniques have been shown to be capable of parts-per-trillion (ppt) level detection of gaseous analytes.[1, 2] In the realm of solid spectroscopy, PAS has been used for condensed phase sample interrogation and depth profiling in layered samples.[3] This versatility makes PAS one of the premier chemical sensing technologies. The development of high-power radiation sources and more sophisticated electronics, including sensitive microphones and digital lock-in amplifiers, has allowed for significant advances in PAS. Furthermore, photoacoustic (PA) detection of infrared absorption spectra using modern tunable lasers offers several advantages, including simultaneous detection and discrimination of numerous molecules of interest.[4]

Photothermal spectroscopy encompasses a group of highly sensitive methods that can be used to detect trace levels of optical absorption and subsequent thermal perturbations of the sample in gas, liquid or solid phases. The underlying principle that connects these various spectroscopic methods is the measurement of physical changes (i.e., temperature, density, or pressure) as a result of a photo-induced change in the thermal state of the sample. In general, photothermal methods are classified as indirect methods for detection of trace optical absorbance, because the transmission of the light used to excite the sample is not measured directly. Examples of photothermal techniques include photothermal interferometry (PTI), photothermal lensing (PTL), photothermal deflection (PTD), and photoacoustic spectroscopy. The

different types of photothermal spectroscopy share the same basic physical processes. A sample under study is illuminated by an optical excitation source, usually a tunable laser, which is intensity modulated by mechanical or electronic means.[5-8] Light from the excitation source is absorbed at a characteristic rate by each sample and leads to a unique response that enables spectroscopy. After illumination, the molecules of the sample undergo a period of relaxation from excited states which produces a rise in temperature in the sample and deformation of the heated surface.[9] As the sample heats it also transfers heat to the adjacent matter (i.e., boundary layer).[10] The boundary layer can be more sample, a substrate, or a fluid. Sample heating drives photothermal phenomena and produces the physical responses measured by the aforementioned techniques. In comparison to other photothermal techniques, which measure the refractive index using combinations of probe sources and detectors, PAS measures the pressure wave produced by sample heating. The rate of heating in the sample and surrounding areas vary at the modulation frequency of the intensity modulated excitation source. When a periodic modulation scheme is chosen, a periodic signal is generated. When the sample is gaseous, or has a gaseous boundary layer, the pressure fluctuations are measurable with a traditional microphone or an interferometer. When the sample is a solid or liquid, the expansion and contraction of the surface in synch with the excitation modulation can be measured with a piezoelectric transducer or an interferometer.[11, 12]

In 1994, the introduction of the quantum cascade laser (QCL) by Bell Labs[13] changed the prospects of laser photoacoustics and, in general, infrared spectroscopy. Since that time, continuing and aggressive evolution has been occurring. The QCL has matured to a level at which numerous companies can produce gain material for laser systems both in the United States and abroad. Along with this production, several companies have produced laser systems that are suitable for spectroscopic purposes. These sources have had a dramatic impact on PA research due to their wide tuning over pertinent regions in the infrared. Over the past 9 years, we have evaluated QCL technology in the implementation of these sources in our miniaturized PA gas sensor platforms.[14] To date, we have demonstrated that widely tunable QCL sources can achieve full spectroscopic discrimination of gas and solid phase analytes, due to their large tuning ranges. Furthermore, these sources operating in low-duty cycles, have demonstrated that PAS based on lock-in amplification can still be performed and indeed shows great promise.[3, 4, 15, 16] Here, we review our most recent PA gas sensing research employing a quasi-continuous wave (QCW) QCL and compare results obtained using this source with previously reported results using pulsed QCLs. We have also employed this QCW source in a standoff PA spectroscopy experiment. This capability is demonstrated with the measurement of the PA spectra of 1,3,5-trinitroperhydro-1,3,5-triazine (RDX) at a standoff range of 1 m.

2. EXPERIMENTAL

Figure 1 depicts a block diagram of the basic elements required for a photoacoustic gas sensor. The pressure waves detected in PAS are generated directly by the absorbed fraction of the modulated or pulsed excitation beam. Therefore, the signal generated from a photoacoustic experiment is directly proportional to the absorbed incident power. Shifting from traditional PA cell-based PAS to a standoff method requires modification to the experimental design. The components remain largely the same, with the exception of the amplifying PA cell and the microphone used to measure the pressure fluctuations. Instead, an interferometer is employed to measure the physical response of the excited system at a standoff distance. Figure 2 depicts a block diagram of the basic elements used in standoff PA measurements.
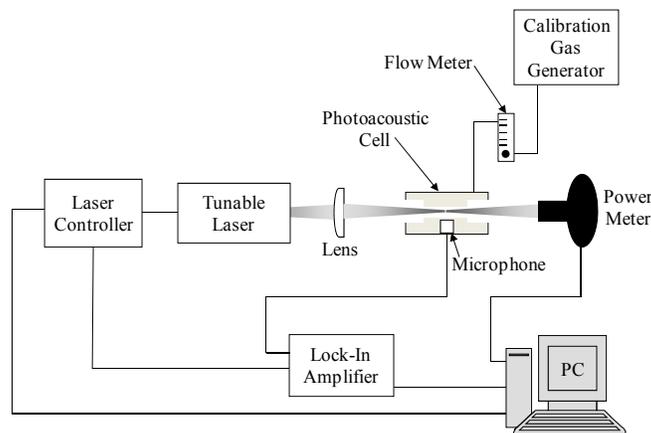
Figure 1. Schematic diagram of a general photoacoustic gas sensor system.
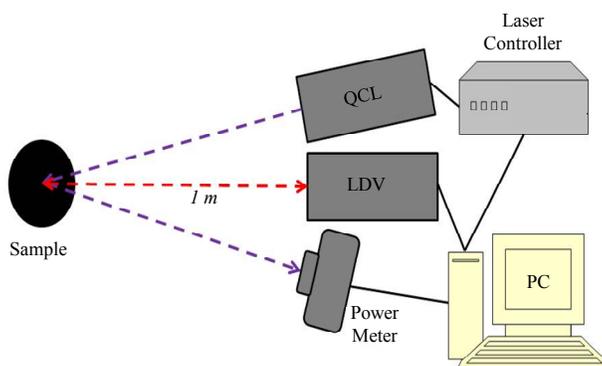
Figure 2. Schematic diagram of the standoff photoacoustic sensing setup. The experiments described herein were all performed at a standoff distance of 1 m with both the excitation source and the LDV at that distance from the target.

2.1 Reagents and Materials

RDX was obtained from Cerilliant. The Cerilliant standard was packaged in acetonitrile (ACN) and used as received unless otherwise noted. Aluminum substrates were purchased from ACT Test Panel Technologies. The substrates were used as received.

2.2 Quantum Cascade Laser

A broadly tunable, quasi-continuous wave (i.e., high duty cycle pulsed operation, typically ~50%) external cavity (EC)-QCL (Pranalytica, Inc. MonoLux-80-CW) was employed as the excitation source for the sensing systems. The QCW laser produced a train of pulses at a high repetition rate (1 MHz). An external modulation envelope could be applied to the train of pulses producing modulated packets of pulses. Alternatively, the laser could be driven externally to produce pulses at lower repetition rates (down to 10s of Hz). The laser was fully self-contained and required only standard AC power and external computer control to operate. The QCL was continuously tunable from 8.733 μm to 6.974 μm (1145 cm^{-1}–1434 cm^{-1}) and had a spectral resolution of 0.001 μm (0.156 cm^{-1}). For the gas sensing experiments, a compact chiller (Solid State Cooling Systems Oasis 150) operated at 17 ºC was used for laser cooling. The laser was driven externally with a transistor-transistor logic (TTL) level (0-5 V, High Z, rising edge synchronization) external drive signal source (Tektronix AFT 3022B) connected to the laser head via a Bayonet Neill–Concelman (BNC) connector. A 5.0 V,

21.6 kHz TTL signal provided an average optical power of 2.70 (±0.05) mW at the center (peak) wavelength. When the laser was driven by the externally supplied pulses, the user had direct control of the laser operation. For the standoff experiments, the QCL operated at room temperature with passive cooling. The laser output was modulated by an externally supplied TTL signal. The modulation was imposed on the internal high frequency (1 MHz) drive signal. A function generator (Tektronix AFG 3022B) was connected to the laser head via a BNC connector to allow for external modulation. A 5.0 V, 5.0 kHz TTL signal resulted in 50% modulation and provided an average optical power of 68 (±2) mW at the peak wavelength. The laser system was equipped with a red guide laser for ease of alignment.

The transmitted laser power was measured with a power meter (Ophir Optronics Nova II) equipped with a thermal head (Ophir Optronics 3A). These measurements allowed for normalization of the photoacoustic signal for any residual drift associated with the excitation source.

2.3 MEMS-Scale Photoacoustic Cell

A MEMS-scale differential photoacoustic cell was fabricated to meet our design specifications[17] by Infotonics Technology Center, Inc. The differential technique employs two resonator tubes, both housing a microphone (Knowles FG-23629), but with radiation directed only through one to generate a photoacoustic signal. The microphones possessed similar responsivities, which allowed for subtraction of the reference microphone signal from the photoacoustic microphone signal. This allowed for the removal of noise elements that were present in both resonant chambers, such as external vibrations.

The influence of cell geometry on the photoacoustic signal has been discussed elsewhere.[1, 18, 19] Briefly, the cell consisted of two 8.5 mm long open resonators having square cross sections, each with a diameter of 0.93 mm. The resonator was flanked on both sides by a buffer volume (acoustic filter), which provided noise suppression. The resonator length was twice that of the buffer volume and the diameter of the buffer volume was at least three times that of the resonator. To further suppress gas flow noise, the buffer volumes were each connected by a tube to gas input and output acoustic filters (Figure 3(A)).
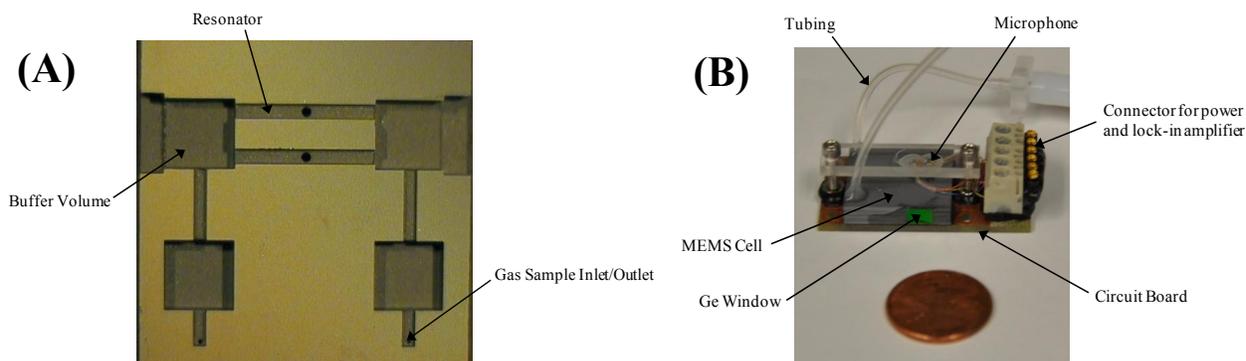
Figure 3. (A) Photograph of the internal structure of the MEMS-scale photoacoustic cell. (B) Photograph of the MEMS-scale photoacoustic cell used when collecting data.

The cell had two germanium windows (Edmund Optics NT47-685), which were attached to the buffer volumes on either side of the photoacoustic resonator with epoxy. Tygon® tubing was connected to the buffer volumes to allow for gas sample inlet and outlet flow. The MEMS-scale photoacoustic cell was mounted on a printed circuit board, which allowed for wiring the microphones to a power supply (AA battery) and a lock-in amplifier (via modified BNC cables). Figure 3(B) is a photograph of the complete MEMS-scale photoacoustic cell package.

2.4 Vapor Sample Generation

The trace gases were generated using a calibration gas generator (Owlstone Nanotech OVG-4). Nitrogen was used as the carrier gas. The gas source was a gravimetrically certified permeation tube (HRT-010.00-3026/40 (acetone)). The acetone tube was placed in a calibration oven held at a constant temperature of 40 °C. The permeation rate at this temperature for acetone was 1,114 ng/min. Varying calibrated flow rates of the nitrogen carrier gas from 50 mL/min to 1000 mL/min governed the concentration of the analyte of interest. The concentration range for the analyte is limited by the permeation tube and the permissible flow rates of the calibration gas generators. Poly (tetrafluoroethylene) (PTFE) tubing was used to connect the gas generator to the sample inlet of the photoacoustic cell. A flow controller and a relief valve were placed in line between the gas generator and the photoacoustic cell to ensure a constant flow rate of 60 mL/min through the cell. This was done to reduce flow noise.

2.5 Data Acquisition (Vapor)

The signals detected by both the photoacoustic and reference microphones were extracted using the differential voltage input on a lock-in amplifier (Stanford Research Systems SR530) with a time constant of 3 s operating at the pulse frequency of the laser or the external modulation frequency of the function generator. LabVIEW (National Instruments, version 2012) was used to create a virtual instrument (VI) to read and record the voltage outputs from the lock-in amplifier under various conditions directly to a personal computer (PC). The VI was programmed to collect the X (in-phase), Y (quadrature), R (amplitude) and θ (phase angle) components of the photoacoustic signal. Photoacoustic spectra were obtained by holding the laser pulse frequency constant while scanning the laser wavelength range. This allowed for the determination of the wavelength having the maximum analyte absorbance in this region. 100 measurements were made at each increment, and a mean value was calculated and recorded for the subsequent construction of a photoacoustic spectrum. To estimate the limit of detection (LOD), the laser pulse frequency and wavelength having the maximum photoacoustic absorbance signal were held constant and the gas generator flow rate was ramped, which produced decreasing sample concentrations. Mean values and standard deviations of 100 points at a given concentration were calculated. The background signal, attributed to the absorbance of laser radiation by the cell windows and walls, was also measured. This background signal was subtracted from the mean photoacoustic signal measured at each concentration. These values were used to prepare a linear regression with which the LOD could be calculated by taking three times the standard deviation (3σ) of the background and dividing it by the slope of the linear function.

2.6 Laser Doppler Vibrometer

For ranged PAS measurements, a laser Dopper vibrometer (Polytec CLV-2534), was the detector. The LDV can be considered a sophisticated Michelson interferometer that calculates the PA system response by measuring the total change in optical path length traveled by a helium neon (HeNe) laser beam that is reflected off the surface of the solid sample. The intersection point of the HeNe beam, solid sample, and excitation laser are carefully aligned to maximize overlap. This alignment is affected because the LDV measures more than the surface change; the difference in path length measured by the LDV is sensitive enough to record changes in the index of refraction that occur due to boundary gas layer heating next to the excitation point on the surface of the sample. LDV measurements are made by examining the interference of the probe beam as it is recombined with a reference beam at a photodiode in the LDV.

Measurements taken with the LDV cannot discriminate between signal generated by physical changes in path length from expansion and contraction of the analyte surface and virtual path length changes arising from variations in the index of refraction of the boundary gas layer produced by temperature and pressure fluctuations. We assume that the signals are in phase and occur at the same repetition rate as the intensity modulation of the excitation beam. The measured signal of the LDV is completely dependent on the reflection of the HeNe probe beam from the surface of the sample. Reflected light must be collected in sufficient amounts to perform any measurements.

PA signal is produced at the exact frequency of modulation used in the excitation of the system. This facilitates the use of a fast Fourier transform (FFT) to isolate the PA signal from the background noise. Software and the digital signal analyzer hardware included with the LDV were sufficient for the purposes of the experiments detailed in this work.

2.7 Sample Configuration (Standoff)

Sample configuration and preparation are important to experimental design and characterization in standoff PAS experiments because signal produced by the LDV is wholly dependent on the reflected probe beam. This dictates careful control over the alignment between the probe beam and sample in the experimental setup. Samples were constructed from two components, a thin layer of the energetic material deposited onto a larger substrate. The two layer sample is attached to a kinematic mirror mount which enables the alignment of the reflected probe beam and the LDV.

The explosive RDX was used to investigate the utility of interferometric measurement of the PA effect at range. 500 $\mu g/cm^2$ of the explosive material was deposited onto an aluminum substrate using a drop-on-demand inkjet printer (MicroFab Technologies Inc.). Drop-on-demand inkjet printing was selected over other methods, such as spray deposition or dropcasting, because of the desire to maximize uniformity of the analyte.[20-25] Drop-on-demand sample preparation has been shown to be an effective way to produce uniform samples of controlled quantities for investigation. The MicroFab system is an unmodified commercial off-the-shelf unit that has been previously shown to produce highly repeatable results with very low relative standard deviations of less than 2%.[23, 26] This sample preparation method allows for the minimization of sample variance as a contributing factor to experimental uncertainty.

2.8 Instrumentation

All Fourier transform infrared (FTIR) absorbance spectra were collected using a Thermo Scientific Nicolet 6700 FTIR spectrometer equipped with a potassium bromide (KBr) beamsplitter and a mercury cadmium telluride (MCT)-A (narrow band – 650 cm^{-1} cutoff) detector. A long-path gas cell (Pike Technologies) accessory was used to collect infrared spectra of gaseous samples. Each spectrum was acquired at a resolution of 1.0 cm^{-1} averaging 100 scans. A GladiATR[TM] (Pike Technologies) accessory was used to collect infrared spectra of solid samples using attenuated total reflectance (ATR). Each spectrum was acquired at a resolution of 2.0 cm^{-1} averaging 100 scans.

3. RESULTS AND DISCUSSION

3.1 Spectroscopic Data

Laser photoacoustic spectra were collected for acetone (gas) and RDX (solid). The intensity normalized spectra are provided in Figure 3. All spectra were collected as the laser was continuously tuned from 7.00 μm to 8.70 μm (1428 cm^{-1}–1150 cm^{-1}), in 0.01 μm (1.5 cm^{-1}) increments. Acetone has known absorption features in this region, assigned to carbon—carbon and carbon—oxygen stretching vibrations.[27, 28] RDX has known absorption features in this region, assigned to nitrogen—nitro stretching vibrations, carbon—hydrogen out of plane bending vibrations, and nitrogen—carbon—nitrogen stretching vibrations.[29] For both species, there is very good agreement between the photoacoustic and FTIR spectra. There are differences in relative peak intensity between the photoacoustic spectra collected for acetone and RDX and the spectra collected with the FTIR. These relative differences likely stem from background sources not eliminated during the background collection. The difference between the spectra are minor and the peaks required for substance identification are clearly reproduced in the photoacoustic measurements.
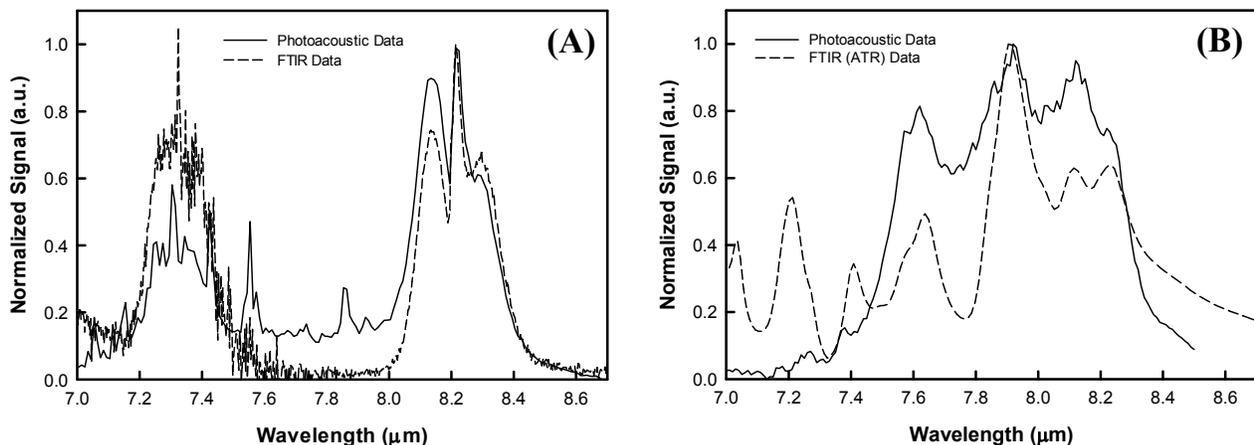
Figure 4. Measured laser photoacoustic spectrum of (A) acetone (gas) and (B) RDX (solid) compared to FTIR reference spectrum.

3.2 Vapor Sensor Responsivity

Photoacoustic gas sensor limits of detection were determined for acetone. Figure 4 illustrates the sensor response as a function of analyte concentration measured at the absorbance maximum (relative to the laser wavelength range). The 3σ limit of detection was determined to be 0.172 ppm for acetone. The results exhibit excellent linearity with a correlation coefficient (R^2) of 0.9961.
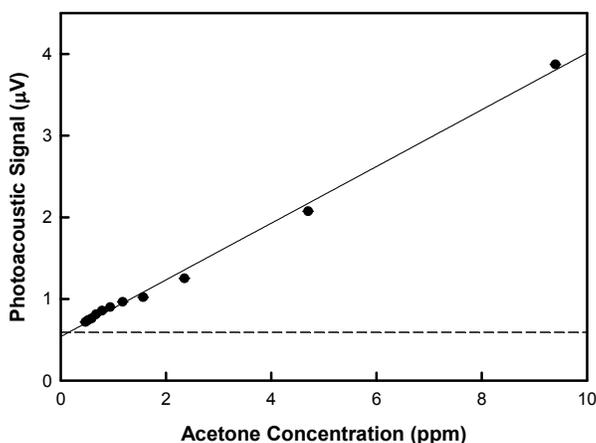
Figure 5. Photoacoustic sensor response as a function of acetone concentration. Error bars represent one standard deviation. The dashed line represents three standard deviations (3σ) of the background signal. A linear function has been fit to the data.

As a measure of the effectiveness of this sensing platform, we considered the National Institute for Occupational Safety and Health (NIOSH) recommended threshold exposure limit value (TLV) for acetone.[30] The TLV for chemical substances is defined as a concentration in air, typically for inhalation or skin exposure. For acetone, the TLV is 250 ppm (value averaged over 10 h). In this report, we have achieved a detection limit well below the suggested value. These results attest to the effectiveness of this MEMS-scale photoacoustic sensing platform.

We have previously reported a LOD for acetone using a similar MEMS-scale photoacoustic sensor platform, in which we employed another commercially available pulsed EC-QCL.[4] In comparison, we have achieved a better LOD here using the QCW QCL driven by externally supplied pulses. It should be noted that the average optical power output for the QCW QCL was greater than that of the previously employed QCL model and we did observe more noise or background signal using the QCW QCL, which ultimately increased the detection limit.

4. CONCLUSION

We have successfully demonstrated the use of a MEMS-scale photoacoustic sensing platform for trace vapor detection. We have evaluated a variety of QCLs in this platform allowing for detection limits in the ppb range and we believe that this sensor platform is an important step toward the development of a man-portable prototype. The availability of continuously tunable QCLs having a broad wavelength tuning range makes this an attractive approach for a variety of applications. Employing multiple continuously tunable QCLs having different center wavelengths in a PA sensor would provide a broad wavelength tuning range, allowing for increased molecular discrimination and simultaneous detection of several molecules of interest.

We have also been successful at demonstrating a standoff PAS platform for the detection of an explosive material deposited on a surface. Our results illustrate the capability of this method for detection of hazards at a distance and without the need for a PA cell. We are working towards decreasing background noise in an effort to optimize the sensitivity of the methodology. Future investigation is required in the examination of limits of detection for the method, as well as determination of the limits to the standoff capability.

5. REFERENCES

[1]   Bijnen, F. G. C., Reuss, J., Harren, F. J. M., "Geometrical optimization of a longitudinal resonant photoacoustic cell for sensitive and fast trace gas detection." Rev. Sci. Instrum. 67, 2914 (1996).
[2]   Nagele, M., Sigrist, M. W., "Mobile laser spectrometer with novel resonant multipass photoacoustic cell for trace-gas sensing " Appl. Phys. B 70, 895 (2001).
[3]   Holthoff, E. L., Marcus, L. S., Pellegrino, P. M., "Quantum Cascade Laser Based Photoacoustic Spectroscopy for Depth Profiling Investigations of Condensed-Phase Materials." Appl. Spectrosc. 66, 987 (2012).
[4]   Holthoff, E., Bender, J., Pellegrino, P., Fisher, A., "Quantum Cascade Laser-Based Photoacoustic Spectroscopy for Trace Vapor Detection and Molecular Discrimination." Sensors 10, 1986 (2010).
[5]   Rosencwaig, A., Gersho, A., "Theory of photoacoustic effect with solids." J. Appl. Phys. 47, 64 (1976).
[6]   Kinney, J. B., Staley, R. H., "Applications of photoacoustic spectroscopy." Ann. Rev. Mater. Sci. 12, 295 (1982).
[7]   Patel, C. K. N., Tam, A. C., "Pulsed optoacoustic spectroscopy of condensed matter." Rev. Mod. Phys. 53, 517 (1981).
[8]   Tam, A. C., "Applications of photoacoustic sensing techniques." Rev. Mod. Phys. 58, 381 (1986).
[9]   Nowacki, W., [Thermoelasticity], Addison-Wesley, Reading, MA, (1962).
[10]   Fetter, A. L., Walecka, J. D., [Theoretical Mechanics of Particles and Continua]. Dover, Mineola, NY, (2003).
[11]   Jackson, W., Amer, N. M., "Piezoelectric photoacoustic detection: theory and experiment." J. Appl. Phys. 51, 3343 (1980).
[12]   Marcus, L. S., "Standoff Laser Interferometric Photoacoustic Spectroscopy for the Detection of Explosives." Ph.D. Thesis, University of Mississippi (2012).
[13]   Faist, J. *et al.*, "Quantum Cascade Laser." Science 264, 553 (1994).
[14]   Holthoff, E. L., Marcus, L. S., Pellegrino, P. M., "Toward the Realization of a Compact Chemical Sensor Platform using Quantum Cascade Lasers." Proc. SPIE 9467, 94672Q (2015).
[15]   Holthoff, E. L., Heaps, D. A., Pellegrino, P. M., "Development of a MEMS-Scale Photoacoustic Chemical Sensor Using a Quantum Cascade Laser." IEEE Sens. J. 10, 572 (2010).
[16]   Holthoff, E. L., Marcus, L. S., Pellegrino, P. M., in *2013 IEEE Sensors*. IEEE, Baltimore, MD, pp. 1-4 (2013).

[17]   Polcawich, R. G., Pellegrino, P. M., US Patent 7304732 (2003).

[18]   Miklos, A. *et al.*, "Improved photoacoustic detector for monitoring polar molecules such as ammonia with a 1.53 mu m DFB diode laser." AIP Conf. Proc., 126 (1999).

[19]   Schill, J. F., Holthoff, E. L., Pellegrino, P. M., "Predicting the Resonant Frequency of Photoacoustic Cells with Side Branches." IEEE Sens. J. 15, 1336 (2015).

[20]   Holthoff, E. L., Farrell, M. E., Pellegrino, P. M., "Standardized sample preparation using a drop-on-demand printing platform." Sensors 13, 5814 (2013).

[21]   Yasuda, K., Woodka, M., Polcha, M., Pinkham, D., "Reproducible deposition of trace explosives onto surfaces for test standards generation." RDER-NV-TR-265, Night Vision, Science and Technology Division: Fort Belvoir, VA (2010).

[22]   Holthoff, E. L., Farrell, M. E., Pellegrino, P. M., "Investigating a drop-on-demand microdispener for standardized sample preparation." Proc. SPIE 8358, 83580V (2012).

[23]   Windsor, E. *et al.*, "Application of inkjet printing technology to produce test materials of 1,3,5-trinitro-1,3,5-triazcyclohexane for trace explosive analysis." Anal. Chem. 82, 8519 (2010).

[24]   Bloom, A. N., Gillen, G., Najarro, M., Windsor, E., "Inkjet printed explosive standards." Abstr. Pap. Amer. Chem. Soc. 237, 204 (2009).

[25]   Windsor, E., Gillen, G., Najarro, M., "ANYL 96-use of drop-on-demand inkjet printing technology." Abstr. Pap. Amer. Chem. Soc. 236, (2008).

[26]   Englmann, M., Fekete, A., Gebefugi, I., Schmitt-Kopplin, P., "The dosage of small volumes for chromatographic quantifications using a drop-on-demand dispenser system." Anal. Bioanal. Chem. 388, 1109 (2007).

[27]   Olmstead, M. A., Amer, N. M., Kohn, S., "Photothermal Displacement Spectroscopy: An Optical Probe for Solids and Surfaces." Appl. Phys. A 32, 141 (1983).

[28]   McMurry, J., [Organic Chemistry], Brooks/Cole, Pacific Grove, CA, 5th ed., (1999).

[29]   Infante-Castillo, R., Pacheco-Londono, L., Hernandez-Rivera, S. P., "Vibrational spectra and structure of RDX and its 13C- and 15N-labeled derivatives: A theoretical and experimental study." Spectrochim Acta A Mol Biomol Spectrosc 76, 137 (2010).

[30]   "Chemical Sampling Information: Acetone." www.OSHA.gov (February 26, 2010).

1 (PDF)	DEFENSE TECHNICAL INFORMATION CTR DTIC OCA
2 (PDF)	DIRECTOR US ARMY RESEARCH LAB RDRL CIO L IMAL HRA MAIL & RECORDS MGMT
1 (PDF)	GOVT PRINTG OFC A MALHOTRA

3
(PDF)
	US ARMY RESEARCH LAB
	RDRL SEE
	  V ATKINSON
	RDRL SEE E
	  E HOLTHOFF
	  P PELLEGRINO